

---

---

GENERAL EXPERIMENTAL  
TECHNIQUES

---

---

## A Solar Spectromagnetograph

I. E. Kozhevator\*, V. N. Obridko\*\*, E. A. Rudenchik\*\*,  
N. P. Cheragin\*, and E. H. Kulikova\*

\*Radiophysical Research Institute, Bol'shaya Pecherskaya ul. 25, Nizhni Novgorod, 603600 Russia

\*\*Institute of Terrestrial Magnetism, Ionosphere, and Propagation of Radiowaves, Russian Academy of Sciences,  
Troitsk, Moscow oblast, 142092 Russia

Received February 15, 2001; in final form, April 28, 2001

**Abstract**—A new solar spectromagnetograph for measuring the full magnetic-field vector and line-of-sight velocities is described. A new version of a polarization analyzer ensuring parallel measurements of six polarization components of spectral lines is considered. The spectromagnetograph allows the use of any algorithms for obtaining the magnetic fields vector, in particular, the Babcock algorithm and the Fourier transform technique. The sensitivity of the instrument for the longitudinal and transverse magnetic field is  $\sim 3\text{--}5$  and  $\sim 20\text{--}30$  G, respectively, and  $\sim 10$  m/s for the line-of-sight velocities.

### 1. INTRODUCTION

Detailed knowledge of magnetic structures is important for understanding solar phenomena, since the magnetic field determines the morphology of the structures in the solar atmosphere and is an energy source for solar flares. Information on the magnetic field vector in the photosphere makes it possible to estimate the vertical component of the electric current, which plays an important role in the corona heating, and enables one to estimate the energy stored in the magnetic field of the corona as a result of such currents.

The magnetic field vector can be determined by various methods, but the most reliable and precise data are obtained from observations of the Zeeman effect in solar spectral lines. In this case, in order to determine the magnetic field vector, it is necessary to measure all polarization parameters of the radiation at a single or several wavelengths of the magnetically sensitive lines. Measurements must be performed at each spatial point of the sun disc under study in a time comparable to the time scale of the developing solar processes.

This paper is the first one of a series devoted to the development of a solar magnetograph based on modern techniques for receiving, analyzing, and processing optical data. Here, we compare filter-based and spectrographical schemes for measuring the radiation polarization characteristics and substantiate ways for modifying the second scheme. A new version of the polarization analyzer, which ensures simultaneous measurements of six polarization components of a spectral line, is considered. The problems and methods of calibration of the new spectromagnetograph will be treated in the next work.

### 2. COMPARISON OF SCHEMES FOR MAGNETIC FIELD MEASUREMENTS

In order to investigate the dynamics of magnetic processes, we need a four-dimensional data array (file) including two spatial, one spectral, and one time coordinate in six versions corresponding to six states of the polarization analyzer. The absence of sufficient resources for parallel measurements of the entire data array leads to the necessity of sacrificing the simultaneousness for one or several measured parameters.

One of the widespread schemes for magnetic fields measurements includes an tunable optical filter, an adjustable polarization analyzer, and a two-dimensional CCD array placed in the solar image plane [1, 2]. The main advantage of this system is that data are obtained simultaneously for all points of the image. However, recording different spectral components of the profile of a magnetically active line and radiation polarization requires sequential measurements. Estimates show that wavelength tuning and successive measurements with different polarization states result in decreased accuracy ( $30\text{--}60$  m/s) in line-of-sight velocity measurements and in an error in magnetic field measurements of  $30\text{--}300$  G.

In addition, because of the low spectral resolution of optical filters, observations are often restricted to measurements only in two spectrum regions of a line wing. Because of this, data can be unambiguously interpreted only within the framework of the simplest model of the solar atmosphere, which hardly conforms with the reality.

Another magnetograph scheme uses a diffraction spectrograph with a long entrance slit as a selective spectral element [3, 4]. In this case, the receiving CCD array is located in the spectrum image plane. Such a scheme has a high spectral resolution and ensures

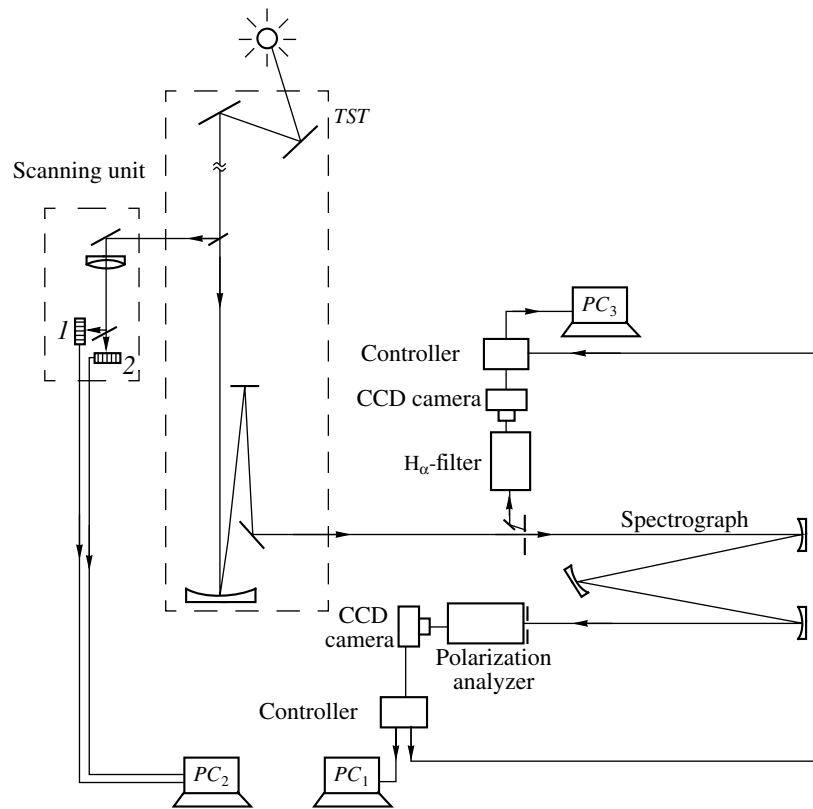


Fig. 1. Functional diagram of the spectromagnetograph on the tower solar telescope.

simultaneous recording of the intensity over the entire spectrum and along one of the spatial coordinates, allowing us to unambiguously interpret the measurement data. However, since the spectrum fluctuations in slit spectrographs are usually higher than those for the filters, this advantage hardly translates into a gain in the accuracy. In addition, the factor of simultaneousness is lost both for the second spatial coordinate because of the necessity for scanning the solar image along it and for the spectral polarization states. Nevertheless, the situation can still be corrected. As a rule, the maximum number of resolved spectral elements over a line profile is within 20–30. This means that no more than 3–5% of the CCD array resolution along one coordinate is used.

As an obvious conclusion, it is necessary to design a device for parallel analysis with respect to the polarization states, which makes it possible to simultaneously record six polarization components of a spectrum. In this case, the time instability of the spectrum loses all significance, because the measurements corresponding to all of the spectrum points are strictly simultaneous for all polarization components. Moreover, this solution reduces the duration of the analysis.

The comparison of two design versions allows us to conclude that, at the current technological level, the spectromagnetograph is somewhat more suitable for

practical implementations than the filter magnetograph design. However, after the development of a system for precise locking to the spectrum of the filter characteristics at each step of its tuning to the line profile and after an increase in the resolution of optical filters, in our opinion, filter magnetographs will be able to compete with spectromagnetographs.

### 3. GENERAL OPTICAL LAYOUT OF THE SPECTROMAGNETOGRAPH

The spectromagnetograph for parallel measurement of the spectral and polarization characteristics of magnetically active lines was designed on the basis of the IZMIRAN optical solar telescope. Its block diagram is shown in Fig. 1. The general system includes a tower solar telescope (TST), a grating spectrograph, a polarization analyzer, two CCD cameras, two controllers, a scanning unit, an H $\alpha$  filter, and three personal computers (PC).

The dispersion of the spectrograph in the second-order spectrum, which is used during the magnetograph's operation, is 0.8 Å/mm. The spectrograph has mirror-type jaws at the entrance slit. The size of the output slit, which is also the entrance slit of the polariza-

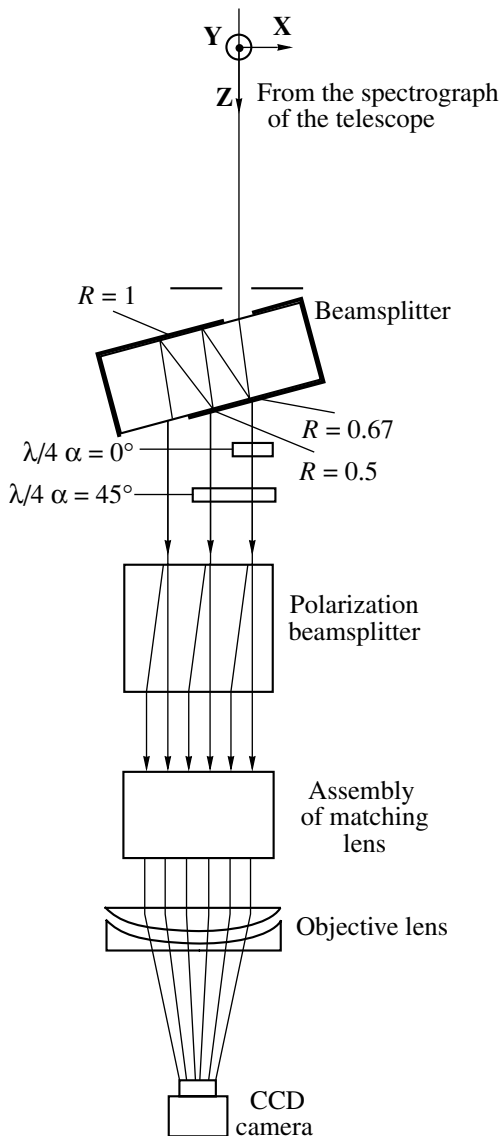


**Fig. 2.** Optical diagram of the parallel-type polarization analyzer.

tion analyzer, is  $20 \times 1.5$  mm. The polarization analyzer is described in detail in Section 4.

Commercial CCD cameras (Proscan, Germany) are used in the system as photodetectors. The number of pixels in the CCD array is  $1024 \times 1024$ , and their size is  $14 \times 14$   $\mu\text{m}$ . The readout rate is 6–10 frame/s. The dark noise and the maximum signal levels correspond to 430 and 16 384 units, respectively. The controller ensures signal recording in a digital 16-bit format. A possibility of mutual synchronization of CCD cameras is provided.

The wide-band guide of the telescope [5, 6] serves as a scanning unit. In order to avoid mechanical movements of the guide's photosensor unit during scanning

over the solar disc, two mutually perpendicular linear CCD arrays 1 and 2 are used in this device.

The  $H_{\alpha}$  filter used in the optical arrangement is an interference–polarization filter (Halle, Germany) transmitting the solar radiation at a wavelength of  $6562.8 \text{ \AA}$  ( $H_{\alpha}$ ).

The TST forms an image of the solar disc 168 mm in diameter on the entrance slit of the spectrograph. The solar radiation transmitted through the spectrograph is directed to the polarization analyzer, which forms six bands of the spectrum region selected corresponding to six polarization states. The intensity in each of these bands is recorded by the first CCD camera. Subsequent data recording is performed with the help of a personal computer,  $PC_1$ .

Scanning along one of the spatial coordinates of the active area is carried out using the scanning unit, whose operation is controlled with a personal computer,  $PC_2$ . The program developed ensures an automatic guidance on any point of the solar image specified by coordinates in a spherical or rectangular system, scanning over the tracer grid, and absolute referencing of the coordinate system, which is fixed to the guide's photosensors, to solar coordinate systems. Moreover, as a result of the action of the wide-band guide in a frequency band of 1–100 Hz, the total value of the solar image motion decreases by a factor of 3–5, and the component related to microseisms is suppressed to the noise level of the tracking system.

The solar radiation reflected by the mirror-like jaws of the spectrograph entrance slit passes through the filter used for constructing a solar image in the  $H_{\alpha}$  hydrogen line. Tracking the image in the  $H_{\alpha}$  line yields prompt information on flares in the chromosphere and ensures more precise referencing of the observation data to spatial solar coordinates, because chromospheric images are more contrasted than photospheric ones.

The use of the slit channel makes it possible to substantially compensate for the drawback of the spectrography technique associated with the necessity of scanning along one of the spatial coordinates. Simultaneous recording of the solar radiation intensity of the active area and the slit position on this area ensures accurate determination of the slit location for all exposures recorded. This also allows us to take into consideration the displacements caused by the sun image motion in the subsequent data analysis.

The image is read out by the second CCD camera and stored by the  $PC_3$ . This computer links the measurement data to the coordinates of the active area under study. Subsequently, it is suggested to develop a program taking into account the geometrical distortions associated with the position of the active area on the solar disc, displacements of the active area with respect to the slit position as a result of solar rotation, and image defocusing.

#### 4. PARALLEL-TYPE POLARIZATION ANALYZER

In Section 2, we noted the high importance of designing a parallel-type polarization analyzer. This device is necessary, when a spectrograph and a low-frequency camera are used as a spectral element and a detector, respectively. If a step-by-step analyzer (with time modulation) is used in this case, then a spectral line may be appreciably shifted in a time required for running all six polarization positions, directly resulting in errors in Zeeman effect measurements.

Step-by-step analyzers have been originally developed for magnetographs in which photomultipliers are used as detectors. In recent years, there have been attempts to transform a step-by-step analyzer into a partially parallel one by forming two parallel channels with orthogonal linear polarization in the optical system [7]. In photography measurement methods (parallel readout), so-called mosaic polarization analyzers that can be regarded as prototypes of parallel analyzers were used [8].

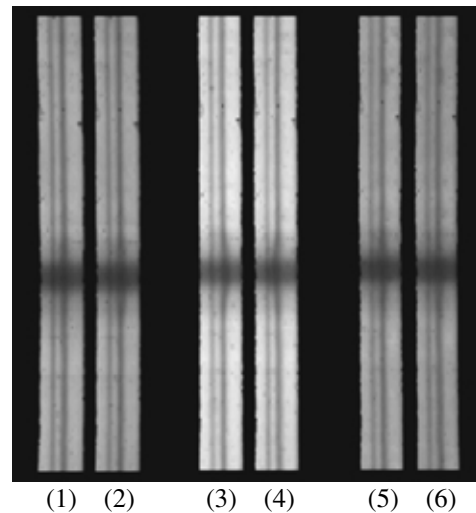
The advent of CCD arrays became the basis for creating fully parallel-type analyzers. However, for some time, this process was delayed by the absence of efficient calibration techniques allowing to compare the intensities in different polarizations when simultaneously detecting images with a large number of elements. With the development of mathematical methods for solving inverse problems, it became possible to accurately compare light–electric characteristics of CCD arrays [9], thus clearing the way for the application of parallel polarization analyzers.

Figure 2 shows the optical diagram of an entirely parallel-type polarization analyzer. The system contains a slit, a beamsplitter, two quarter-wavelength plates, a polarization beam splitter, a unit of matching lenses, and an objective lens.

As was mentioned above, the spectrograph output slit and the analyzer entrance slit coincide. In accordance with the spectrograph's dispersion and slit dimensions, a spectrum band with a height of 20 mm and a spectral width of  $\sim 1.2 \text{ \AA}$  is incident on the front plane of the beamsplitter.

The spatial beamsplitter is designed for forming three maximally identical beams with minimal distortion of the initial polarization. The front plane of the beamsplitter (except for the entrance window) has a reflecting coating with a reflectivity  $R = 1$ . The rear face has a reflecting coating with  $R = 0.67$  on a third of its length,  $R = 0.5$  on another one third, while there is no coating at all on the remaining one third.

The beamsplitter is oriented at a  $1/8$  angle to the optical axis. This angle is a result of a trade-off between the obtainment of sufficiently separated beams (the distance between them is  $\sim 6 \text{ mm}$ ) and a minimum distortion of the radiation polarization characteristics. The reflecting layers ensure polarization-isotropic characteristics of the beamsplitter in a band of  $\pm 200 \text{ \AA}$ . Note that the subsequent calibration of the polarization ana-



**Fig. 3.** Radiation intensity of the solar spectrum in six different polarizations in the vicinity of the solar spectral line Fe I with  $\lambda = 6302.5 \text{ \AA}$  (right lines) and the telluric oxygen line with  $\lambda = 6302.8 \text{ \AA}$  (left lines). The radiation corresponds to the cross section of the active area in the sunspot.

lyzer makes it possible to take into account the nonidentity of rays (in the beams) and distortions in the polarization properties; at the same time, the aforementioned requirements should not be considered superfluous.

The directions of the polarization axes of the first quarter-wavelength plate coincide with the axes of the coordinate system. The directions of the polarization axes of the second  $\lambda/4$  plate are turned with respect to those of the first plate clockwise by an angle of  $45^\circ$  in the  $XY$ -plane.

The polarization beamsplitter made of spar is a beam-separating crystal element, from which beams with orthogonal linear polarizations emerge in parallel to each other. The polarizations of the ordinary and extraordinary waves are directed along the  $Y$  and  $X$  axes, respectively.

In order to reduce the entire image to a size corresponding to the CCD array, an assembly of matching lenses and an exit objective lens are introduced into the optical system. With their involvement, three pairs of reduced images are brought into coincidence in a common plane on the CCD array of the camera.

After passing through the beamsplitter, the light beam is divided into three beams of equal intensities. The first one passes through two quarter-wavelength plates, the second beam, through one plate, and the third beam is transmitted unimpeded. Subsequently, all three beams fall onto the polarization beam splitter, where they are transformed into six parallel beams corresponding to different linear polarization states and shifted with respect to each other in the  $X$ -direction with a step of 2 mm.

Figure 3 shows the spectrum images in six different polarizations in the vicinity of the Fe I solar line ( $\lambda = 6302.5 \text{ \AA}$ , the Lande factor is 2.5) and the line of atmo-

spheric oxygen ( $\lambda = 6302.8 \text{ \AA}$ ). The latter serves as a reference line in line-of-sight velocity measurements. The radiation corresponds to the cross section of the active region in a sunspot.

The combination of the quarter-wavelength plates with the polarization beam splitter in our system is sufficient for one to obtain the necessary set of Stokes parameters. At the perfectly manufactured quarter-wavelength plates, the intensity values in each of the six beams are described by the expressions

$$J + Q, \quad (1) \quad J - V, \quad (4)$$

$$J - Q, \quad (2) \quad J + U, \quad (5)$$

$$J + V, \quad (3) \quad J - U. \quad (6)$$

Their numbers correspond to the band numbers in Fig. 3, and  $J$ ,  $Q$ ,  $V$ , and  $U$  correspond to the Stokes parameters according to the conventional notation [10].

As known, four independent linear equations are sufficient for calculating four parameters. Nevertheless, in order to obtain the parameters determining the magnetic field vector, it is preferable to have these six relations. On the one hand, the greater part of the array area is unutilized. On the other hand, the three most important Stokes parameters ( $Q$ ,  $V$ , and  $U$ ) can be easily derived from relations (1)–(6) by appropriate subtractions, making it possible to eliminate any possible additive errors (interferences, noises). This error elimination technique is similar to the modulation method for noise suppression, which is widely used in the sequential analysis.

In the actual system, the reflection coefficients of the elements of the spatial beamsplitter differ from the specified values, and distortions of the polarization characteristic of the radiation introduced by the optics of both the polarization analyzer and the spectrograph exist. Moreover, the light transmission efficiency of the system may be different for each pixel, since it depends on the individual sensitivity of a pixel and on the presence of dust and contaminations on optical elements, including the jaws of the entrance slit of the spectrograph and sensitive elements of the CCD camera. As a result of the effect of these factors distorting an ideal pattern, each pixel has its own polarization matrix.

Hence, the general problem of calibration of magnetographs and, especially, that of the type under consideration, is at least as important as the development and creation of the optico-electronic system itself. However, this part of the problem is so wide in scope and topical that it deserves special consideration.

## CONCLUSIONS AND OUTLOOKS

The spectromagnetograph with parallel spectral and polarization analysis of radiation described in this

paper was mounted on the IZMIRAN tower solar telescope between August and September 2000 and was test-operated. The spectromagnetograph ensures a sensitivity of  $\sim 3\text{--}5 \text{ G}$  in measurements of the longitudinal magnetic field,  $\sim 20\text{--}30 \text{ G}$  for the transverse field,  $\sim 10 \text{ m/s}$  for line-of-sight velocities and, in addition, permits the use of any algorithms for measurements of the magnetic field vector, such as the Babcock algorithm and the Fourier transform method [11]. This is an advantage of a spectromagnetograph over the filter magnetograph.

An important feature of the parallel polarization analyzer designed for the spectromagnetograph is that it is entirely static. It contains no controllable elements implying mechanical movements and feeding of electric signals. Therefore, it is much more stable as compared to mechanical and electro-optic modulators and has an almost unlimited service life.

The spectromagnetograph described will be fully brought into operation in the 2001 season and will be used in permanent observations of the full vector of the magnetic field and line-of-sight velocities in the solar atmosphere.

## ACKNOWLEDGMENTS

This work was supported in part by the Federal Research and Technical program "Astronomy" (Sections 1.5.4.5 and 1.5.5.1).

## REFERENCES

1. Wang, H., Dencer, C., Spirock, T., *et al.*, *Sol. Phys.*, 1998, vol. 183, p. 1.
2. Milkey, D.L., Canfield, R.C., LaBronte, B.J., *et al.*, *Sol. Phys.*, 1996, vol. 168, p. 229.
3. Jones, H.P., Duvall, Th.L., Harvey, J.W., *et al.*, *Sol. Phys.*, 1992, vol. 139, p. 211.
4. Grigoryev, V.M., Kobanov, N.I., and Skomorovsky, V.I., *Proc. SPIE*, 1994, vol. 2265, p. 373.
5. Kozhevato, I.E., Rudenchik, E.A., Cheragin, N.P., *et al.*, *Prib. Tekh. Eksp.*, 2000, no. 1, p. 120.
6. Kozhevato, I.E., Rudenchik, E.A., Cheragin, N.P., *et al.*, *Prib. Tekh. Eksp.*, 2000, no. 1, p. 125.
7. Grigoryev, V.M. and Kobanov, N.I., *Astron. Astrophys., Suppl. Ser.*, 1997, vol. 122, p. 293.
8. Mogilevskii, E.I., Veller, A.E., and Val'd-Perlov, V.M., *Dokl. Akad. Nauk SSSR*, 1954, vol. 95, p. 957.
9. Rudenchik, E.A., Kozhevato, I.E., Cheragin, N.P., *et al.*, *Opt. Spektrosk.*, 2001, vol. 90, no. 1, p. 127.
10. Zirin, H., *The Solar Atmosphere*, Waltham, Mass.: Blaisdell, 1966. Translated under the title *Solnechnaya atmosfera*, Moscow: Mir, 1969.
11. Ioshpa, B., Obridko, V., and Kozhevato, I., *Sol. Phys.*, 1996, vol. 164, p. 373.